Insulin receptor substrate-1 deficiency drives a proinflammatory phenotype in *KRAS* mutant lung adenocarcinoma

Heather E. Metz[a,b,c], Julia Kargl[c,d], Stephanie E. Busch[c], Kyoung-Hee Kim[c], Brenda F. Kurland[e,f], Shira R. Abberbock[e], Julie Randolph-Habecker[g], Sue E. Knoblaugh[h], Jay K. Kolls[i], Morris F. White[j], and A. McGarry Houghton[c,h,k,l,1]

[a]Department of Medicine, Fred Hutchinson Cancer Research Center, Seattle, WA 98109; [b]Department of Pathology, Fred Hutchinson Cancer Research Center, Seattle, WA 98109; [c]Clinical Research Division, Fred Hutchinson Cancer Research Center, Seattle, WA 98109; [d]Institute of Experimental and Clinical Pharmacology, Medical University of Graz, 8036 Graz, Austria; [e]University of Pittsburgh Cancer Institute, University of Pittsburgh School of Medicine, Pittsburgh, PA 15261; [f]Department of Biostatistics, University of Pittsburgh Graduate School of Public Health, Pittsburgh, PA 15261; [g]Experimental Histopathology Shared Resource, Fred Hutchinson Cancer Research Center, Seattle, WA 98109; [h]Department of Veterinary Biosciences, The Ohio State University, Columbus, OH 43210; [i]Department of Pediatrics, University of Pittsburgh School of Medicine, Pittsburgh, PA 15261; [j]Division of Endocrinology, Boston Children's Hospital, Boston, MA 02115; [k]Human Biology Division, Fred Hutchinson Cancer Research Center, Seattle, WA 98109; and [l]Division of Pulmonary and Critical Care, University of Washington, Seattle, WA 98195

Edited by C. Ronald Kahn, Joslin Diabetes Center Harvard Medical School, Boston, MA, and approved June 10, 2016 (received for review February 5, 2016)

Insulin receptor substrate-1 (IRS-1) is a signaling adaptor protein that interfaces with many pathways activated in lung cancer. It has been assumed that IRS-1 promotes tumor growth through its ability to activate PI3K signaling downstream of the insulin-like growth factor receptor. Surprisingly, tumors with reduced IRS-1 staining in a human lung adenocarcinoma tissue microarray displayed a significant survival disadvantage, especially within the Kirsten rat sarcoma viral oncogene homolog (*KRAS*) mutant subgroup. Accordingly, adenoviral Cre recombinase (AdCre)-treated *LSL-Kras/Irs-1*$^{fl/fl}$ (*Kras/Irs-1*$^{-/-}$) mice displayed increased tumor burden and mortality compared with controls. Mechanistically, IRS-1 deficiency promotes Janus kinase/signal transducers and activators of transcription (JAK/STAT) signaling via the IL-22 receptor, resulting in enhanced tumor-promoting inflammation. Treatment of *Kras/Irs-1*$^{+/+}$ and *Kras/Irs-1*$^{-/-}$ mice with JAK inhibitors significantly reduced tumor burden, most notably in the IRS-1-deficient group.

insulin receptor substrate-1 | lung | adenocarcinoma | Kras

Lung cancer continues to be the leading cause of cancer deaths worldwide (1), and in the United States it accounts for more than 160,000 deaths per year with 5-y survival rates of just ∼15% (2). Lung cancer is a heterogeneous disease that is typically subdivided into small-cell lung cancer (SCLC) and non–small-cell lung cancer (NSCLC), which constitute ∼15% and 85% of cases, respectively. NSCLC is further subclassified into multiple histologic subtypes, including lung adenocarcinoma (L-ADCA; ∼60%) and lung squamous cell carcinoma (L-SCCA; ∼20%) (3). L-ADCAs frequently possess a driving mutation in a key oncogene, such as Kirsten rat sarcoma viral oncogene homolog (KRAS) and the EGF receptor (EGFR). Whereas *EGFR* mutant cancers can be addressed with novel targeted therapies, *KRAS* mutant tumors remain largely untargetable (4).

Numerous studies have examined the impact of a specific driving mutation on the function of a particular signaling pathway, though none have addressed the role of insulin receptor substrate-1 (IRS-1) (5). Of the numerous proteins involved in pathway signaling, IRS-1 is somewhat unique in that it interfaces with many different pathways, including the PI3K, extracellular signal regulated kinase (MEK/ERK), and Janus kinase/signal transducers and activators of transcription (JAK/STAT) signaling pathways (6, 7). IRS-1 is afforded this promiscuity as a result of possessing numerous binding domains, including an N-terminal pleckstrin homology (PH) domain, a phosphotyrosine binding (PTB) domain, and a carboxy terminus with multiple serine and tyrosine phosphorylation sites (6). IRS-1 is a signaling adaptor protein best known for mediating canonical signaling from both the insulin receptor (IR) and the insulin-like growth factor receptor (8). The majority of research investigating the function of IRS proteins has naturally been performed in the setting of glucose metabolism and diabetes in metabolically active tissues (muscle and adipose). In this context, IRS-1 has been appropriately characterized as a positive effector of growth factor (9, 10). However, the impact of IRS-1 on pathway activity in cancer cells, where aberrant signaling is frequently encountered, has not been adequately addressed.

An emerging concept in cancer biology is the role of the tumor microenvironment (TME) in tumor progression (11), and the role of aberrant pathway signaling in sculpting the TME (12, 13). Immune cells represent a major component of the TME, frequently comprising over half of the cells in resected tumor specimens. It has become evident that inflammatory responses increase tumor initiation and progression, because immune cells are capable of supplying tumors with the growth factors, cytokines, and reactive oxygen species required to promote proliferation, survival, angiogenesis, invasion, and metastasis (14, 15). The mechanisms by which cancers generate tumor-promoting microenvironments must be further explored to identify novel therapeutic agents that address the TME.

Given the prominent role of IRS-1 in signaling pathways commonly hyperactive in L-ADCA, we undertook an independent study of this protein within the adenocarcinoma subtype. Surprisingly, we identified a counterparadigmatic and prohost role for IRS-1 specifically in *KRAS* mutant L-ADCA via alterations in cancer cell signaling that subsequently impacted the cellular composition of the TME.

Significance

Kirsten rat sarcoma viral oncogene homolog (*KRAS*) mutant lung adenocarcinoma remains an intractable lung cancer subtype for which efficacious targeted therapies do not exist. This study identified a subpopulation of *KRAS* mutant lung adenocarcinoma with reduced insulin receptor substrate-1 (IRS-1) content and showed that this group is particularly amenable to Janus kinase/signal transducers and activators of transcription (JAK/STAT) inhibition. This finding is the first definitive report of a prohost role for IRS-1 in a solid tumor malignancy in humans. Furthermore, the data supports a novel role for IRS-1 in the sculpting of immune cell composition within the tumor microenvironment.

Author contributions: H.E.M., J.K.K., M.F.W., and A.M.H. designed research; H.E.M., J.K., S.E.B., K.-H.K., J.R.-H., and A.M.H. performed research; H.E.M., B.F.K., S.R.A., J.R.-H., S.E.K., and A.M.H. contributed new reagents/analytic tools; H.E.M., B.F.K., S.R.A., and A.M.H. analyzed data; H.E.M. and A.M.H. wrote the paper; H.E.M., J.K.K., and M.F.W. conceptualized the study; J.R.-H. and S.E.K. provided software; and A.M.H. supervised and conceptualized the study.

The authors declare no conflict of interest.

This article is a PNAS Direct Submission.

[1]To whom correspondence should be addressed. Email: houghton@fredhutch.org.

This article contains supporting information online at www.pnas.org/lookup/suppl/doi:10.1073/pnas.1601989113/-/DCSupplemental.

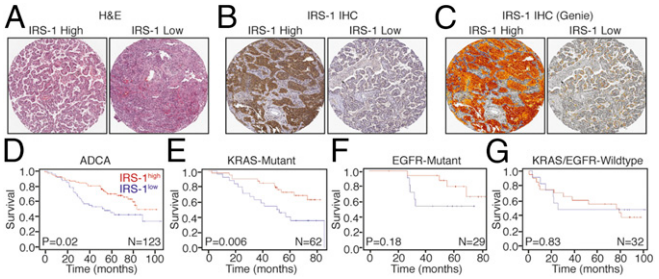

Fig. 1. IRS-1 predicts patient survival in L-ADCA. (*A* and *B*) Representative images of IRS-1^{low} (H-score <130) and IRS-1^{high} (H-score >130) human L-ADCA TMA sections stained for (*A*) H&E and (*B*) IRS-1. (*C*) Example of tumor compartment-specific quantification of IRS-1 staining using Aperio Genie. (*D*–*G*) Kaplan–Meier estimates of overall survival for the (*D*) entire lung adenocarcinoma cohort ($n = 123$, $P = 0.02$, (*E*) *KRAS* mutant cases ($n = 62$, $P = 0.006$), (*F*) *EGFR* mutant cases ($n = 29$, $P = 0.18$), and (*G*) Non-*KRAS*, non-*EGFR* mutant cases ($n = 32$, $P = 0.83$). All *P* values determined from log-rank tests.

Results

KRAS Mutant, IRS-1^{low} Lung Adenocarcinoma Subgroup Displays Reduced Patient Survival. To evaluate associations between IRS-1 protein content and L-ADCA patient outcomes, we stained and analyzed a human tissue microarray (TMA) consisting of 135 primary tumor specimens that had been annotated for KRAS and EGFR mutation status, and for which survival data were available. Immunohistochemistry staining of IRS-1 was quantified using an Aperio Genie system. H-scores were generated by assessing the IRS-1 staining intensity within the tumor compartment. Examples of H&E-stained, IRS-1-stained, and Genie overlay images from cases displaying abundant (IRS-1^{high}) or reduced IRS-1 staining (IRS-1^{low}) are shown in Fig. 1 *A*–*C*.

As a continuous variable, IRS-1 expression did not predict overall survival (OS) (hazard ratio = 0.99, 95% CI 0.98–1.00, $P = 0.16$). Threshold effects were explored using recursive partitioning, identifying an H-score cut point of 130 (Fig. 1*D*; log-rank test *P* value = 0.02). Classification by IRS-1 did not appear a proxy for other patient or tumor characteristics (Table S1). Evaluated in subgroups by mutational status, the prognostic signal for dichotomized IRS-1 appeared to be driven by tumors with KRAS mutations (Fig. 1*E*). In these patients, the median OS was 50 mo for IRS-1^{low} (95% confidence interval 30–84 mo) and 131 mo for IRS-1^{high} (71–131 mo). EGFR mutant, and EGFR and KRAS wild-type (not KRAS or EGFR mutant) subgroups did not demonstrate IRS-1 as a strong prognostic factor (Fig. 1 *F* and *G*). The effect of IRS-1 persisted in a multivariable model. Smoking status (current/former/never, $P = 0.18$), smoking consumption (pack years, $P = 0.55$), and age ($P = 0.96$) were not associated with overall survival in univariate or multivariate models (Table S1). Therefore, the primary multivariable model included pathologic stage and sex. In this model, the hazard ratio for dichotomized IRS-1 was 1.8 (95% CI 1.1–3.1): patients with IRS-1^{low} tumors had a hazard of death nearly twice that of those with IRS-1^{high} (Wald test *P* value = 0.03).

***Kras/Irs-1*$^{-/-}$ Mice Display Increased Tumor Burden and Decreased Survival.** To further interrogate the phenotype identified in the human TMA study, we generated *Lox-Stop-Lox-Kras/Irs-1*$^{+/+}$ and *Lox-Stop-Lox-Kras/Irs-1*$^{fl/fl}$ mice on a pure 129.SvJ genetic background. Mice were treated intratracheally with adenoviral Cre recombinase (AdCre) at 8 wk of age to activate mutant Kras expression and to delete Irs-1 (Fig. 2*D*). AdCre-treated *Lox-Stop-Lox-Kras/Irs-1*$^{+/+}$ mice will be denoted as *Kras/Irs-1*$^{+/+}$ and AdCre-treated *Lox-Stop-Lox-Kras/Irs-1*$^{fl/fl}$ mice will be denoted as *Kras/Irs-1*$^{-/-}$. The mice were subsequently studied over a time course ranging from 4 to 20 wk post-AdCre. Similar to the findings in human L-ADCA, Kaplan–Meier survival curves demonstrated inferior survival for *Kras/Irs-1*$^{-/-}$ mice compared with *Kras/Irs-1*$^{+/+}$ control mice ($P < 0.0001$; Fig. 2*A*). *Kras/Irs-1*$^{-/-}$ mice displayed a median survival of 14 wk, compared with a median survival of 20 wk in the *Kras/Irs-1*$^{+/+}$ control group. Additionally, tumor burden was quantified at 4, 8, and 12 wk post-AdCre (Fig. 2 *B* and *C*). Statistically significant increases in tumor burden were observed in IRS-1-deficient mice at the 8- and 12-wk time points, representing a doubling and tripling of the tumor burden identified in control mice. Although we assessed for local and distant metastases, we were unable to identify any in either group.

In attempts to distinguish between differential rates of apoptosis vs. cellular proliferation as the cause of increased tumor burden in *Kras/Irs-1*$^{-/-}$ mice, we performed cleaved caspase-3 and K_i-67 staining (Fig. 2 *E* and *F*). We were unable to identify tumor cells staining positively for cleaved caspase-3 (CC3) in either group, and did not quantify apoptosis further. Quantification of K_i-67 staining demonstrated a statistically significant increase in tumor cell proliferation in the *Kras/Irs-1*$^{-/-}$ group (Fig. 2*G*). Therefore, the increased tumor burden in *Kras/Irs-1*$^{-/-}$ mice results from enhanced proliferation, and not decreased apoptosis.

Increased Neutrophilic Inflammation in *Kras/Irs-1*$^{-/-}$ Mice. Surprisingly, the most striking initial phenotypic difference apparent in the *Kras/Irs-1*$^{-/-}$ mice was elevated inflammatory cell content in the bronchoalveolar lavage (BAL) fluid (Fig. 3 *A* and *B*). Further investigation revealed robust increases in macrophage and neutrophil content (Fig. 3 *A* and *B*). At 12 wk, neutrophils were approximately fivefold higher in *Kras/Irs-1*$^{-/-}$ BAL, and Ly6G staining revealed the presence of tumor-associated neutrophils (Fig. 3*C*). Quantitative PCR (qPCR) was performed on lung tissue to assess differential expression of CC and CXC chemokines known to recruit myeloid lineage cells to the TME. *Kras/Irs-1*$^{-/-}$ mice displayed increases in most of these chemokines compared with *Kras/Irs-1*$^{+/+}$ mice (Fig. 3*D*). Specifically, we identified significant increases in CCL-2, -3, -4, and CXCL-1, -2, and -5, consistent with the BAL cellular content data. To validate the qPCR findings at the protein level, we performed ELISA analysis for CCL-2, CCL-4, CXCL-1, and CXCL-2. Consistent with the qPCR data, *Kras/Irs-1*$^{-/-}$ mice possess increased amounts of all four chemokines in their BAL fluid, compared with *Kras/Irs-1*$^{+/+}$ mice (Fig. 3*E*).

To verify a tumor-promoting role for tumor-associated neutrophils, we treated both cohorts of mice with a neutrophil-depleting Ly6G antibody (clone 1A8), which reduced both tumor-associated neutrophilic inflammation and tumor growth (Fig. S1), consistent

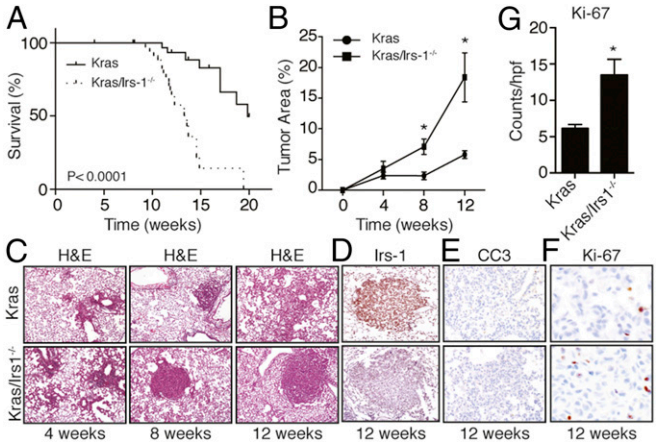

Fig. 2. Increased tumor burden and mortality in *Kras/Irs-1*$^{-/-}$ mice. (*A*) Kaplan–Meier estimates of overall survival for AdCre-treated *Kras/Irs-1*$^{+/+}$ ($n = 41$) and *Kras/Irs-1*$^{-/-}$ ($n = 44$) mice. $P < 0.0001$, log-rank test. (*B*) Tumor area percent (percent of lung tissue occupied by tumor) for *Kras/Irs-1*$^{+/+}$ and *Kras/Irs-1*$^{-/-}$ mice at 4, 8, and 12 wk post-AdCre. (*C*) Representative H&E-stained images for *Kras/Irs-1*$^{+/+}$ and *Kras/Irs-1*$^{-/-}$ mice 4, 8, and 12 wk post-AdCre. (*D*–*F*) Representative (*D*) Irs-1, (*E*) CC3, and (*F*) K_i-67 stained images for *Kras/Irs-1*$^{+/+}$ and *Kras/Irs-1*$^{-/-}$ mice at 12 wk post-AdCre. (*G*) Quantification of K_i-67 staining. All $n = 6$ per group. Bars ± SEM. *$P < 0.05$.

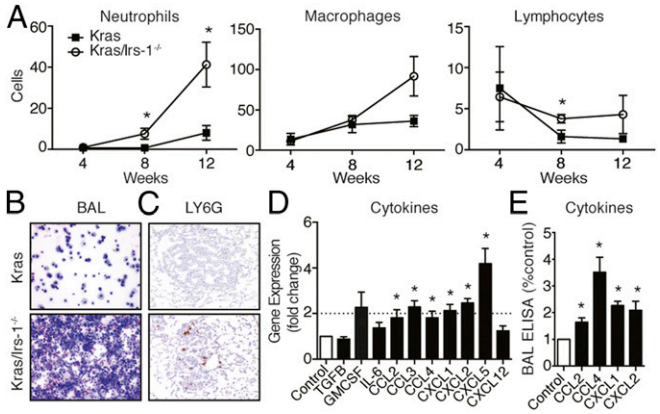

Fig. 3. Increased tumor-associated inflammation in *Kras/Irs-1*$^{-/-}$ mice. (*A*) BAL fluid content of neutrophils, macrophages, and lymphocytes from *Kras/Irs-1*$^{+/+}$ and *Kras/Irs-1*$^{-/-}$ mice at 4, 8, and 12 wk post-AdCre. $n = 6$ per group. (*B*) Representative Hema-3-stained cytospins performed on BAL fluid from *Kras/Irs-1*$^{+/+}$ and *Kras/Irs-1*$^{-/-}$ mice at 12 wk post-AdCre. (*C*) Representative anti-Ly6G (neutrophil marker)-stained sections from *Kras/Irs-1*$^{+/+}$ and *Kras/Irs-1*$^{-/-}$ at 12 wk post-AdCre. (*D*) Real-time PCR values for the listed genes from *Kras/Irs-1*$^{+/+}$ and *Kras/Irs-1*$^{-/-}$ mice at 8 wk post-AdCre. $n = 4$ per group. Results expressed as fold change from *Kras/Irs-1*$^{+/+}$. (*E*) Chemokine expression (pg/mL) in BAL fluid from *Kras/Irs-1*$^{+/+}$ and *Kras/Irs-1*$^{-/-}$ mice at 8 wk post-AdCre. $n = 4$ per group. Results expressed as fold change from *Kras/Irs-1*$^{+/+}$. All bars ± SEM. *$P < 0.05$.

with prior reports (16, 17). Not surprisingly, the impact of anti-Ly6G on tumor burden was greater in the IRS-1-deficient group, in which the tumor microenvironment is enriched in neutrophil content.

IL-22 Is Required for Increased Chemokine Response in IRS-1-Deficient Cancer Cells. To further evaluate the differences in chemokine production observed between *Kras/Irs-1*$^{+/+}$ and *Kras/Irs-1*$^{-/-}$ mice, we generated IRS-1-deficient A549 (KRAS mutant) L-ADCA cells using shRNA approaches. We were not able to observe an increase in cytokine or chemokine production in a microarray study of IRS-1-silenced A549 cells under standard serum conditions (Table S2). We then reasoned that a factor present in the TME, but absent in cultured cancer cells, might be responsible for the in vivo observations in *Kras/Irs-1*$^{-/-}$ mice. Of the factors known to be present within the TME, strong evidence exists to support a role for the Th17 family of cytokines in the amplification of myeloid cell-recruiting chemokines (18). Recently, Chang et al. (19) found that IL-17A-deficient KRAS mutant mice displayed reduced tumor burden, tumor-associated inflammation, and CC and CXC chemokine production in vivo. Therefore, we tested the ability of IL-6, IL-17A, and IL-22 to induce greater CC and CXC chemokine expression from IRS-1-deficient cancer cells in vitro. A549 cells silenced for IRS-1 (shIRS-1) and short hairpin RNA (shRNA) vector control (shCon) were stimulated with the above cytokines and qPCR was performed to assess for differences in cytokine and chemokine production. As expected, IL-6, IL-17, and IL-22 increased cytokine and chemokine expression in A549 cells. However, only IL-22 induced a greater increase in cytokine and chemokine production in IRS-1-silenced cells than it did in shCon cells (Fig. 4*A*). Because survival differences in human L-ADCA were limited to the KRAS mutant group, we repeated these experiments in 201T L-ADCA cells, which harbor WT KRAS alleles. TGF-β was induced by IL-6, IL-17A, and IL-22 treatments, but other cytokines and chemokines were not up-regulated by IRS-1 deficiency in the absence of KRAS mutation (Fig. 4*B*). We were further able to reproduce these findings in the KRAS mutant H460 lung cancer cell line (Fig. 4*J*). Because IRS-1 did not impact patient outcomes in EGFR mutant patients, we repeated these assays in H1650 cells, which are EGFR mutant but KRAS WT. Similar to the findings in KRAS WT 201T cells, H1650 cells did not produce excessive CC/CXC chemokines in response to IL-22 (Fig. 4*L*), further highlighting the requirement for mutant KRAS in this setting.

IL-22 Stimulation Causes Exaggerated pSTAT3 Production in KRAS Mutant, IRS-1-Silenced Cells. IL-22 is a known inducer of JAK/STAT signaling (20). To investigate the impact of IRS-1 deficiency on IL-22-induced JAK/STAT signaling, we treated shIRS-1 and shCon

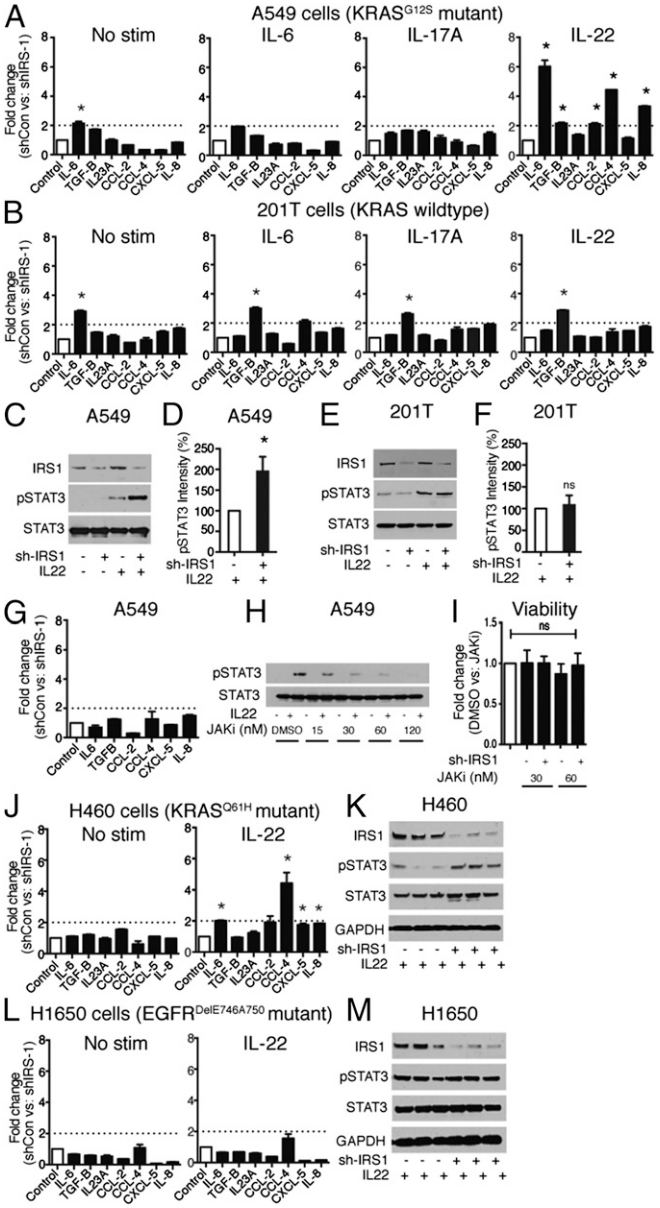

Fig. 4. IRS-1 deficiency enhances IL-22 signaling. (*A* and *B*) Real-time PCR values for the listed genes from lentiviral control (shCon) and IRS-1-silenced (shIRS-1) (*A*) A549 and (*B*) 201T cells treated with IL-6, IL-17A, or IL-22. Results expressed as fold changed in gene expression from shCon values ± SEM. *$P < 0.05$. (*C* and *D*) Western blot and band densitometry ($n = 4$) for shCon and shIRS-1 A549 cells with and without IL-22 stimulation. (*E* and *F*) Western blot and band densitometry ($n = 4$) for shCon and shIRS-1 201T cells with and without IL-22. (*G*) Real-time PCR values for listed genes from shCon and shIRS-1 A549 cells pretreated with a JAK inhibitor (Millipore no. 420099) and stimulated with IL-22. Results expressed as fold change from control values. (*H*) Western blot probed for STAT3 and pSTAT3 from A549 cells treated with a JAK inhibitor over the indicated concentrations and stimulated with IL-22. (*I*) Viability assay comparing DMSO and JAK inhibitor-treated A549 cells. Results expressed as fold change from control values. (*J* and *L*) Real-time PCR values for the listed genes from shCon and shIRS-1 (*J*) H460 and (*L*) H1650 cells treated with IL-22. Results expressed as fold changed in gene expression from control. (*K* and *M*) Western blot for shCon and shIRS-1 (*K*) H460 cells and (*M*) H1650 cells with IL-22 stimulation. All bars ± SEM. *$P < 0.05$.

A549 and 201T cells with IL-22, both in the presence and absence of a JAK inhibitor. As expected, IL-22 stimulation increased the production of pSTAT3 compared with non–IL-22-stimulated control cells, for all conditions (Fig. 4 *C* and *E*). Predictably, the addition of a synthetic JAK inhibitor (Millipore) abrogated pSTAT3 production and cytokine/chemokine induction under all conditions, though it did not impact cellular viability (Fig. 4 *G–I*). Notably, IRS-1-silenced A549 cells (KRAS mutant) displayed an even greater increase in pSTAT3 production upon IL-22 stimulation than did vector control A549 cells (Fig. 4 *C* and *D*). In contrast, IL-22-induced pSTAT3 production was similar in magnitude between IRS-1-silenced and vector control 201T cells (KRAS WT; Fig. 4 *E* and *F*). We were able to reproduce the alterations in pSTAT3 production in an independent KRAS mutant cell line (H460) and an additional KRAS WT cell line (H1650; Fig. 4 *K–M*). To demonstrate that this mechanism was operative in vivo, formalin-fixed, paraffin-embedded (*FFPE*) sections from *Kras/Irs-1*$^{+/+}$ and *Kras/Irs-1*$^{-/-}$ mice were subjected to IHC for pSTAT3 (Fig. 5*A*). Tabulation of the slides confirmed greater pSTAT3 production in *Kras/Irs-1*$^{-/-}$ mice (Fig. 5*B*), compared with controls, thereby validating the in vitro findings with respect to pSTAT3.

IRS-1 Deficiency Prolongs IL-22 Receptor Alpha 1 Half-Life via pGSK-3β Production. The increased production of pSTAT3 by IRS-1-deficient cancer cells compared with control was observed while using an equivalent concentration of IL-22. This finding suggests that the production of pSTAT3 induced by each molecule of IL-22 is greater for IRS-1-silenced cells compared with controls. One possible mechanism that would explain these observations would be a prolongation of the IL-22R half-life in IRS-1-deficient cells. IHC for IL-22 receptor alpha 1 (IL-22RA1) was performed on FFPE sections from *Kras/Irs-1*$^{-/-}$ mice and *Kras/Irs-1*$^{+/+}$ controls. Similar to the findings with respect to pSTAT3, *Kras/Irs-1*$^{-/-}$ tumors displayed greater than twice the IL-22RA1 staining compared with *Kras/Irs-1*$^{+/+}$ controls (Fig. 5 *C* and *D*); to demonstrate this more clearly, IRS-1-silenced and vector control A549 cells were treated with cycloheximide before IL-22 stimulation and subsequent tracking of IL-22RA1 cycling. The IL-22RA1 signal is gradually lost from the membrane as it is internalized following activation, tagged for degradation, and eventually completely absent in the membrane fraction (Fig. 5*E*). Because the cells have been treated with cycloheximide, they are incapable of repopulating the cell surface with new receptor. In contrast, by the conclusion of the experiment in IRS-1-deficient cells, the IL-22RA1 membrane content has been restored, because the receptor has been recycled to the membrane, never having been degraded.

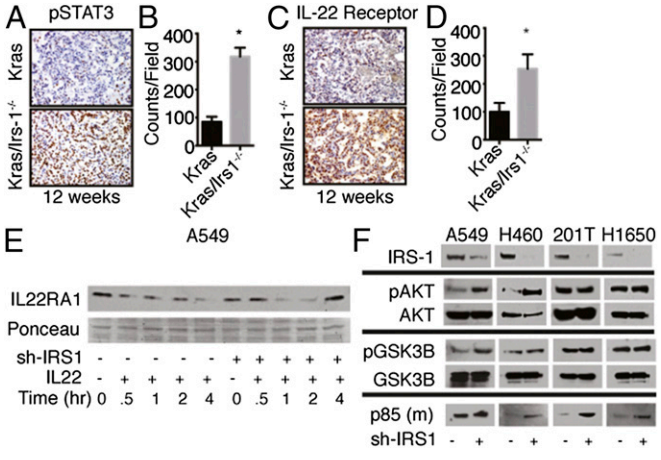

Fig. 5. Increased IL-22RA1 content in IRS-1-silenced cells. (*A*) Representative images and (*B*) quantification for pSTAT3-stained sections from *Kras/Irs-1*$^{+/+}$ and *Kras/Irs-1*$^{-/-}$ mice at 12 wk post-AdCre. $n = 6$ per group. (*C*) Representative images and (*D*) quantification for IL22RA1-stained sections from *Kras/Irs-1*$^{+/+}$ and *Kras/Irs-1*$^{-/-}$ mice at 12 wk post-AdCre. $n = 5$ per group. (*E*) Control and IRS-1-silenced A549 cells were pretreated with cycloheximide before IL-22 stimulation. Western blots probed for IL-22RA1 and p85 were performed on membrane fraction. (*F*) Representative Western blots for the indicated proteins in shCon and shIRS-1 A549, H460, 201T, and H1650 cells. All bars ± SEM. *$P < 0.05$.

Recently, pGSK-3β has been shown to phosphorylate the cytoplasmic tail of IL-22RA1, which inhibits the ability of ubiquitinases to tag the receptor for degradation (21); this results in a prolongation of IL-22RA1 half-life. Because IRS-1 is a homeostatic binding partner of the p85 subunit of PI3K, and well known to impact PI3K signaling, we investigated the impact of IRS-1 deficiency on pAKT and pGSK-3β production in KRAS mutant and KRAS WT cells. IRS-1 silencing had little effect on pAKT and pGSK-3β production in KRAS WT 201T and H1650 cells (Fig. 5*F*). However, IRS-1 deficiency in the presence of mutant KRAS (A549 and H460) actually increased both pAKT and pGSK-3β (Fig. 5*F*). As a signaling adaptor protein, IRS-1 is able to interact with p85 within the cytosol, following phosphorylation by a cell-surface receptor; this is in contrast to the usual receptor tyrosine kinases that interact with p85 near the inner leaflet of the cellular membrane, where lipid substrates are abundant. In the absence of IRS-1, the subcellular location of p85 relocates predominantly to the cell membrane, regardless of KRAS mutational status (i.e., it occurs equally in all cell lines tested; Fig. 5*F*). Similar observations were previously made in adipocytes (22). These data suggest that pAKT and pGSK-3β production is increased when p85 is located nearest to the phosphoinositols, if a continuous signaling mutated protein is present (Fig. S2).

JAK Inhibition Reduces Inflammation and Tumor Burden in *Kras/Irs-1*$^{-/-}$ Mice. Although the increased tumor-associated inflammation and tumor burden identified in *Kras/Irs-1*$^{-/-}$ mice was the result of a multistep process, all of these steps culminated in JAK/STAT activation. Therefore, we administered a JAK1 selective antagonist, AZ-289, and a JAK1/2 antagonist, AZD-1480, to both *Kras/Irs-1*$^{+/+}$ and *Kras/Irs-1*$^{-/-}$ mice. The mice received AZ-289, AZD-1480, or vehicle control via oral gavage 6 d/wk for 3 wk, starting 8 wk post-AdCre. Analysis of the bronchoalveolar lavage fluid inflammatory cell content for both JAK antagonists revealed that *Kras/Irs-1*$^{-/-}$ mice possessed substantially reduced inflammation that was similar in magnitude to that observed in *Kras/Irs-1*$^{+/+}$ mice (Fig. 6 *E* and *F*). Both inhibitors also reduced CC and CXC chemokine expression, as expected (Fig. 6 *G–J*). AZD-1480 and AZ-289 significantly reduced the tumor burden in both cohorts, though the tumor burden was not significantly different for one drug compared with the other (Fig. 6 *A–C*). Mechanistically, JAK inhibition did not induce apoptosis in any treatment group (Fig. S3). Instead, we identified reductions in K_i-67-positive tumor cells in response to both reagents (Fig. 6 *K* and *L*). These results provide evidence that JAK inhibition reduces tumor burden in Kras mutant mice, and is additionally capable of abrogating the enhanced tumor-promoting inflammation afforded by IRS-1 deficiency.

KRAS mutant, IRS-1^{low} Human Lung Adenocarcinomas Contain Increased Myeloid Cell Inflammation. To demonstrate that the proinflammatory phenotype identified in *Kras/Irs-1*$^{-/-}$ mice was present in human disease, we reanalyzed the human lung adenocarcinoma TMA for immune cell content. Specifically, we scored all KRAS mutant cases in our TMA for myeloid cell and lymphocyte infiltration (both on a semiquantitative score from 0 to 3, where absent is 0, mild is 1, moderate is 2, and heavy is 3). These scores were also combined to give a total immune cell content score. KRAS mutant, IRS-1^{low} cancers possessed ∼30% greater content of inflammatory cells, and ∼40% increased myeloid cell infiltration, but no significant difference in lymphoid inflammation was identified, consistent with the findings in the *Kras* mouse model (Fig. S4).

Discussion

We began this study of IRS-1 in lung cancer by identifying that IRS-1-deficient lung adenocarcinomas displayed reduced survival, but that this phenotype was restricted to the *KRAS* mutant

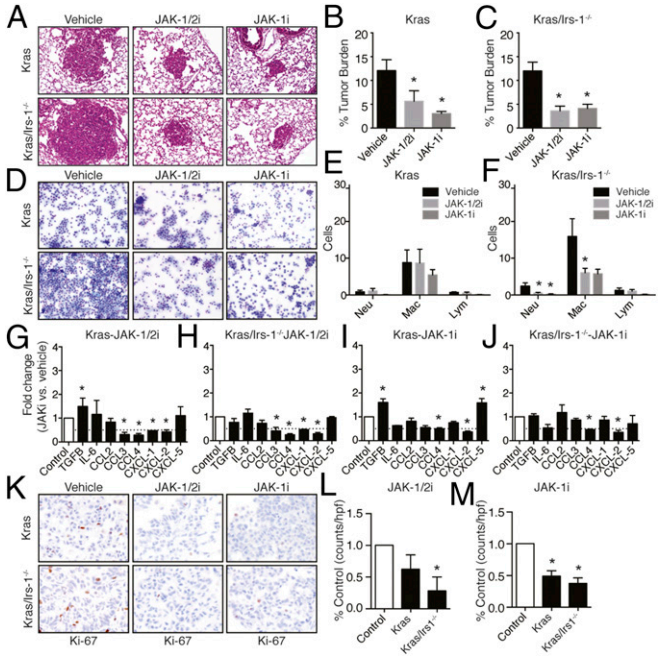

Fig. 6. JAK inhibition reduces tumor burden and inflammation in *Kras/Irs-1*$^{-/-}$ mice. (*A*) Representative H&E-stained sections from *Kras/Irs-1*$^{+/+}$ and *Kras/Irs-1*$^{-/-}$ mice treated with JAK-1/2 inhibitor (AZD-1480), JAK-1 inhibitor (AZ-289), or vehicle control for a total of 3 wk beginning at 8 wk post-AdCre. (*B* and *C*) Tumor area percent (percent of lung occupied by tumor) for (*B*) *Kras/Irs-1*$^{+/+}$ and (*C*) *Kras/Irs-1*$^{-/-}$ drug-treated mice, as above. $n = 6$ per group. (*D*) Representative images and (*E* and *F*) quantification of Hema-3-stained cytospins of BAL fluid from *Kras/Irs-1*$^{+/+}$ and *Kras/Irs-1*$^{-/-}$ drug-treated mice. (*G–J*) Real-time PCR values for the listed genes from (*G*) *Kras/Irs-1*$^{+/+}$ and (*H*) *Kras/Irs-1*$^{-/-}$ drug-treated mice. Results are expressed as fold change from vehicle control ± SEM. $n = 3$ per group. (*K*) Representative images and (*L* and *M*) quantification for K_i-67 stained sections from *Kras/Irs-1*$^{+/+}$ and *Kras/Irs-1*$^{-/-}$ drug-treated mice, as above. $n = 3$–5 per group. All bars ± SEM. *$P < 0.05$.

L-ADCA subtype. Controlled experiments in mice reproduced the phenotype observed in humans and uncovered a proinflammatory phenotype highlighted by enhanced pSTAT3 production, excessive CC and CXC chemokine expression, and consequential increases in inflammatory cell content. We suspect that most, but not all, of the differences in tumor burden were the result of increased tumor-promoting inflammation, because we were able to diminish tumor burden using a neutrophil-depleting antibody, as has been reported several times previously (16, 17). It appears that the enhanced tumor-associated inflammation in IRS-1-deficient tumors functions to drive tumor cell proliferation, as evidenced by increased Ki67 staining in *Kras/Irs-1*$^{-/-}$ tumors. There does not appear to be a role for differential apoptosis here, because apoptosis is rare in the *Kras* model, independent of IRS-1 content.

Mechanistically, IRS-1-deficient cells display an altered subcellular distribution of the PI3K machinery, favoring a plasma membrane location. Under certain circumstances, such as the presence of mutant *KRAS*, abundant PI3K within close proximity to its lipid substrates can enhance PI3K pathway activity, as observed here. In this case, increased pGSK-3β production increased the half-life of IL-22RA1, ultimately causing enhanced pSTAT3 production, CC/CXC chemokine expression, and increased protumor inflammatory cell infiltration.

The importance of the Th17 cytokines IL-17 and IL-22 in solid tumor malignancies has been highlighted by several recent publications (18, 23). Though we were unable to identify a role for IL-17A specifically in the context of IRS-1 deficiency, IL-17A-deficient mice were recently shown to display reduced tumor burden and tumor-associated inflammation in the *LSL-Kras* model used here (19). Notably, IL-22 has recently been shown to play dual roles in cancer (24). Early in the process of tumorigenesis, IL-22 is essential for epithelial cell repair, and actually retards tumor formation. In contrast, in established lesions in proinflammatory colon cancer models, IL-22 drives myeloid cell infiltration and tumor burden via JAK/STAT-mediated amplification of CC/CXC chemokine production, similar to our findings. IL-22 accounts for most, but not all, of the CC/CXC chemokine amplifications identified in *Kras/Irs-1*$^{-/-}$ tumors. Taking into consideration the differences between human and mouse, such as the fact that human lung cancer cell lines rarely express CCL-3 (none of our cell lines did) and that we used IL-8 as a surrogate for CXCL-1 and -2, only CXCL-5 was not reproduced using IL-22 stimulation. Given the complexity of the TME, it is highly likely that there are other factors at play in addition to IL-22. Identifying the mechanistic basis for elevated CXCL-5 production by IRS-1-deficient tumors is an area of active investigation in our laboratory.

To our knowledge, this is the first definitive report of a prohost role for IRS-1 in any human cancer type and is paradigm-shifting in nature. Traditionally, IRS-1 is considered a positive effector of growth factor and presumed to promote tumor growth via PI3K activation, which is likely the case in certain malignancies. Several immunohistochemistry (IHC)-based studies have correlated IRS-1 staining with poor outcomes (25). The only prior study of IRS-1 in human lung cancer reported that 46% of NSCLC cases had diminished IRS-1 content by IHC, though outcomes data were not available (26). Notably, we denoted 38% of L-ADCA on the TMA as being IRS-1^{low}, consistent with the prior study. Taken together, these studies strongly suggest that ∼40% of L-ADCA tumors display reduced IRS-1 content at the protein level. Specifically within the *KRAS* mutant group, 39% of cases were defined as IRS-1^{low}, such that ∼10% of all L-ADCA is comprised of this unique subtype. Furthermore, these findings may explain why initial clinical trials using IGF-1R antagonists have not produced positive results (27). IGF-1R inhibition would be expected to reduce the pTyr-IRS-1 cellular content, which would reduce IRS-1:p85 interaction, because only pTyr-IRS-1 binds to p85. Thus, IGF-1R inhibition may generate a relatively deficient IRS-1 state, which, in the presence of mutant *KRAS*, may produce untoward effects.

Notable limitations of the current study include the fact that the classification of IRS-1^{high} and IRS-1^{low} tumors was based on data-driven criteria. Therefore, external validation will be required before further clinical investigation. Additionally, we have not identified the mechanism by which IRS-1 protein content is reduced in human L-ADCA, though we suspect it is related to neutrophilic inflammation; it is unlikely to be the result of a mutation, because IRS-1 mutations were uncommon in the lung adenocarcinoma TCGA dataset (28). We previously identified a significant correlation between neutrophil elastase (NE) staining and reduced IRS-1 staining on serial sections of 38 human L-ADCAs using IHC (29). In that study, we were also able to show that NE entered tumor cells, which resulted in the elimination of intracellular IRS-1. Since the time of that report, NE has been shown to enter multiple different cancer cell types, including breast cancer (30, 31). NE also enters nonmalignant cells, such as fibroblasts (32) and hepatocytes (33), both of which caused the loss of intracellular IRS-1. It is intriguing to consider a positive feedback loop in which tumor-associated neutrophilic inflammation would lead to IRS-1 degradation via NE activity, with the subsequent reduction in intracellular IRS-1 content driving further recruitment of neutrophils, thereby propagating the cycle.

The results reported here highlight a novel concept with respect to pathway signaling in cancer cells. Whereas the focus of aberrant pathway signaling has logically centered upon hyperactive mutant proteins (KRAS, PIK3CA, BRAF, etc.), this report clearly demonstrates that signaling intermediaries can drastically impact cell behavior when their content is reduced. Signaling intermediates are numerous, and mutated versions of many of these proteins are not frequently encountered. However, relative deficiencies of promiscuous signaling proteins, such as IRS-1, can impact pathway output in a manner that is difficult to predict. *KRAS* mutant, IRS-1^{low} lung adenocarcinomas represent a unique

subtype in which JAK/STAT activation is excessive and drives tumor-promoting inflammation. Because the constellation of events instigated by IRS-1 deficiency culminates in pSTAT3 production, we used JAK inhibitors to show that this tumor subtype is particularly susceptible to this therapeutic strategy. These experiments highlight the role of IRS-1 in lung adenocarcinoma. *KRAS* mutant cancers contain some degree of inherent tumor-associated inflammation due to the ability of mutant *KRAS* to induce cytokines, such as IL-8, through NFκB activation (12). Although there is likely to be some contribution of JAK/STAT activity in sculpting the TME, pathway output is enhanced in IRS-1-deficient tumors. Therefore, JAK inhibition and, more specifically, JAK1 inhibition, eliminates the excessive chemokine production and subsequent inflammation afforded by IRS-1 deficiency, resulting in decreased tumor cell proliferation and tumor burden. Because *KRAS* mutant IRS-1^{low} lung adenocarcinomas represent 10% of all lung adenocarcinomas, JAK inhibition may represent a viable therapeutic option, especially when considering the intractable nature of *KRAS* mutant cancers.

Methods

Mouse Studies. Animal experiments were performed in accordance with approved Institutional Animal Care and Use Committee (IACUC) protocols in a pathogen-free barrier facility at the Fred Hutchinson Cancer Research Center. Mouse models, tissue collection, assessment of mortality, BAL fluid analysis, histology, immunohistochemistry, qPCR analysis of lung tissue, and therapeutic studies are described in detail in *SI Methods*.

In Vitro Studies. Human lung cancer cell lines, IRS-1 silencing, microarray, IL-22 treatment, JAK inhibition, Western blotting, and qPCR analysis are described in *SI Methods*.

Human Tissue Microarray. An L-ADCA cohort on TMA was obtained from the University of Pittsburgh Cancer Institute. The TMA is annotated for *KRAS* mutant, *EGFR* mutant, or WT-*EGFR* and WT-*KRAS* status and survival data. Patient identifiers were removed and the study was considered Institutional Review Board exempt. TMA was stained with an IRS-1 antibody (Santa Cruz no.sc-720) and analyzed using an Aperio Genie system. Experimental details described in *SI Methods*.

Statistical Analysis. Detailed statistical analyses for human TMA study as well as in vitro and in vivo studies are described in *SI Methods*.

ACKNOWLEDGMENTS. We thank AstraZeneca for supplying AZD-1480 and AZ-289. This project was supported by the Sidney Kimmel Foundation (A.M.H.), NIH/National Cancer Institute (NCI) Grant R01CA188341 (to A.M.H.), NIH/NCI Grant P50CA090440 (University of Pittsburgh Cancer Institute Lung Specialized Programs of Research Excellence (SPORE)), a Marie Curie Actions Fellowship (to J.K.), and the Fred Hutchinson Cancer Research Center. This project used the University of Pittsburgh Cancer Institute (UPCI) Tissue and Research Pathology Services, Cancer Information Services Facility, and the Biostatistics Shared Resource Facility, supported in part by NIH Award P30CA047904.

1. Jemal A, et al. (2009) Cancer statistics, 2009. *CA Cancer J Clin* 59(4):225–249.
2. Dubey S, Powell CA (2009) Update in lung cancer 2008. *Am J Respir Crit Care Med* 179(10):860–868.
3. Herbst RS, Heymach JV, Lippman SM (2008) Lung cancer. *N Engl J Med* 359(13):1367–1380.
4. Skoulidis F, et al. (2015) Co-occurring genomic alterations define major subsets of KRAS-mutant lung adenocarcinoma with distinct biology, immune profiles, and therapeutic vulnerabilities. *Cancer Discov* 5(8):860–877.
5. Babur Ö, et al. (2015) Systematic identification of cancer driving signaling pathways based on mutual exclusivity of genomic alterations. *Genome Biol* 16:45.
6. Taniguchi CM, Emanuelli B, Kahn CR (2006) Critical nodes in signalling pathways: Insights into insulin action. *Nat Rev Mol Cell Biol* 7(2):85–96.
7. Yu H, Pardoll D, Jove R (2009) STATs in cancer inflammation and immunity: A leading role for STAT3. *Nat Rev Cancer* 9(11):798–809.
8. White MF (2002) IRS proteins and the common path to diabetes. *Am J Physiol Endocrinol Metab* 283(3):E413–E422.
9. Backer JM, et al. (1992) Phosphatidylinositol 3′-kinase is activated by association with IRS-1 during insulin stimulation. *EMBO J* 11(9):3469–3479.
10. White MF, Yenush L (1998) The IRS-signaling system: A network of docking proteins that mediate insulin and cytokine action. *Curr Top Microbiol Immunol* 228:179–208.
11. Coussens LM, Zitvogel L, Palucka AK (2013) Neutralizing tumor-promoting chronic inflammation: A magic bullet? *Science* 339(6117):286–291.
12. Sparmann A, Bar-Sagi D (2004) Ras-induced interleukin-8 expression plays a critical role in tumor growth and angiogenesis. *Cancer Cell* 6(5):447–458.
13. Ji H, et al. (2006) K-ras activation generates an inflammatory response in lung tumors. *Oncogene* 25(14):2105–2112.
14. Hanahan D, Weinberg RA (2011) Hallmarks of cancer: The next generation. *Cell* 144(5):646–674.
15. Lu H, Ouyang W, Huang C (2006) Inflammation, a key event in cancer development. *Mol Cancer Res* 4(4):221–233.
16. Gong L, et al. (2013) Promoting effect of neutrophils on lung tumorigenesis is mediated by CXCR2 and neutrophil elastase. *Mol Cancer* 12(1):154.
17. Jamieson T, et al. (2012) Inhibition of CXCR2 profoundly suppresses inflammation-driven and spontaneous tumorigenesis. *J Clin Invest* 122(9):3127–3144.
18. Coffelt SB, et al. (2015) IL-17-producing γδ T cells and neutrophils conspire to promote breast cancer metastasis. *Nature* 522(7556):345–348.
19. Chang SH, et al. (2014) T helper 17 cells play a critical pathogenic role in lung cancer. *Proc Natl Acad Sci USA* 111(15):5664–5669.
20. Lejeune D, et al. (2002) Interleukin-22 (IL-22) activates the JAK/STAT, ERK, JNK, and p38 MAP kinase pathways in a rat hepatoma cell line. Pathways that are shared with and distinct from IL-10. *J Biol Chem* 277(37):33676–33682.
21. Weathington NM, et al. (2014) Glycogen synthase kinase-3β stabilizes the interleukin (IL)-22 receptor from proteasomal degradation in murine lung epithelia. *J Biol Chem* 289(25):17610–17619.
22. Tsuji Y, et al. (2001) Subcellular localization of insulin receptor substrate family proteins associated with phosphatidylinositol 3-kinase activity and alterations in lipolysis in primary mouse adipocytes from IRS-1 null mice. *Diabetes* 50(6):1455–1463.
23. McAllister F, et al. (2014) Oncogenic Kras activates a hematopoietic-to-epithelial IL-17 signaling axis in preinvasive pancreatic neoplasia. *Cancer Cell* 25(5):621–637.
24. Huber S, et al. (2012) IL-22BP is regulated by the inflammasome and modulates tumorigenesis in the intestine. *Nature* 491(7423):259–263.
25. Chang Q, Li Y, White MF, Fletcher JA, Xiao S (2002) Constitutive activation of insulin receptor substrate 1 is a frequent event in human tumors: Therapeutic implications. *Cancer Res* 62(21):6035–6038.
26. Han CH, et al. (2006) Clinical significance of insulin receptor substrate-I down-regulation in non-small cell lung cancer. *Oncol Rep* 16(6):1205–1210.
27. Langer CJ, et al. (2014) Randomized, phase III trial of first-line figitumumab in combination with paclitaxel and carboplatin versus paclitaxel and carboplatin alone in patients with advanced non-small-cell lung cancer. *J Clin Oncol* 32(19):2059–2066.
28. Anonymous; Cancer Genome Atlas Research Network (2014) Comprehensive molecular profiling of lung adenocarcinoma. *Nature* 511(7511):543–550.
29. Houghton AM, et al. (2010) Neutrophil elastase-mediated degradation of IRS-1 accelerates lung tumor growth. *Nat Med* 16(2):219–223.
30. Mittendorf EA, et al. (2012) Breast cancer cell uptake of the inflammatory mediator neutrophil elastase triggers an anticancer adaptive immune response. *Cancer Res* 72(13):3153–3162.
31. Gregory AD, Hale P, Perlmutter DH, Houghton AM (2012) Clathrin pit-mediated endocytosis of neutrophil elastase and cathepsin G by cancer cells. *J Biol Chem* 287(42):35341–35350.
32. Gregory AD, et al. (2015) Neutrophil elastase promotes myofibroblast differentiation in lung fibrosis. *J Leukoc Biol* 98(2):143–152.
33. Talukdar S, et al. (2012) Neutrophils mediate insulin resistance in mice fed a high-fat diet through secreted elastase. *Nat Med* 18(9):1407–1412.
34. Jackson EL, et al. (2001) Analysis of lung tumor initiation and progression using conditional expression of oncogenic K-ras. *Genes Dev* 15(24):3243–3248.
35. Dong XC, et al. (2008) Inactivation of hepatic Foxo1 by insulin signaling is required for adaptive nutrient homeostasis and endocrine growth regulation. *Cell Metab* 8(1):65–76.
36. Houghton AM, et al. (2006) Elastin fragments drive disease progression in a murine model of emphysema. *J Clin Invest* 116(3):753–759.
37. Siegfried JM, et al. (1999) Evidence for autocrine actions of neuromedin B and gastrin-releasing peptide in non-small cell lung cancer. *Pulm Pharmacol Ther* 12(5):291–302.
38. LeBlanc M, Crowley J (1992) Relative risk trees for censored survival data. *Biometrics* 48(2):411–425.
39. Du P, Kibbe WA, Lin SM (2008) lumi: A pipeline for processing Illumina microarray. *Bioinformatics* 24(13):1547–1548.
40. Smyth GK (2005) limma: Linear models for microarray data. *Bioinformatics and Computational Biology Solutions Using R and Bioconductor, Statistics for Biology and Health*, eds Gentleman R, Carey V, Huber W, Irizarry R, Dudoit S (Springer, New York), pp 397–420.